Vortex Formation in Dilute Inhomogeneous Bose-Einstein Condensates

B. Jackson, J. F. McCann, and C. S. Adams
Department of Physics, University of Durham, South Road, Durham, DH1 3LE, England
(Received 9 December 1997)

We solve the time-dependent Gross-Pitaevskii in 2D to simulate the flow of an object through a dilute Bose-Einstein condensate trapped in a harmonic well. We demonstrate vortex formation and study the process in terms of the accumulation of phase slip and the evolution of the fluid velocity. [S0031-9007(98)05993-6]

PACS numbers: 03.75.Fi, 67.40.Vs

The origin of drag in quantum liquids is central to the understanding of superfluidity [1]. For a weakly interacting fluid, Bogoliubov showed that macroscopic occupation of the ground state leads to a linear dispersion curve and, hence, superfluidity for motion slower than a critical velocity. However, for liquid helium, the transition to normal flow is observed at a much lower velocity than can be explained by the dispersion curve. This led Feynman [2] to suggest that the onset of dissipation may arise due to vortex shedding, but experimental verification of this idea has been impeded by the two-fluid nature of liquid helium, which complicates quantitative comparison with theory.

The recent experimental discovery of Bose condensation in dilute alkali vapors [3–5] presents a near-perfect system for the study of quantum fluids: The condensates are almost pure and sufficiently dilute so that the interactions can be accurately parametrized in terms of a scattering length. As a result, a relatively simple nonlinear Schrödinger equation (NLSE), known as the Gross-Pitaevskii equation [6], gives a precise description of condensate dynamics. Experiments have confirmed that the NLSE is remarkably accurate in the limit of low temperature [7–9].

Recent experiments have also demonstrated that far-off resonant laser light may be used to split [10], excite [11], trap [12], shape and pierce [13] dilute alkali vapor condensates. The question arises whether such light forces may be used to study the phenomenon of vortex formation, and thereby shed some light on the issue of superfluidity. In this paper, we simulate the motion of an "object" through a dilute atomic condensate. The object corresponds to the potential barrier produced by a far-off resonant blue-detuned laser beam. The laser beam is focused at the center of the trap producing a toroidal condensate in 3D [13]. A quasi-2D configuration could be realized with the laser propagating along the minor axis of an oblate spheroid condensate. We solve the time-dependent NLSE in 2D and show that vortices are produced when the object is translated faster than a critical speed. For homogeneous fluid flow past an impenetrable cylindrical obstacle, it has been shown that the critical velocity is proportional to the speed of sound [14,15]. However, for the inhomogeneous condensate and penetrable object treated here, the situation is considerably more complex because both the critical velocity and the sound speed are functions of position. Consequently, the conditions for vortex creation depend on the shape of the condensate and the form of the object potential. For example, even for low object speeds, vortices are created towards the edge of the condensate due to the decrease in the speed of sound.

The 2D NLSE in the xy plane may be written as

$$i\partial_t\psi = (-\nabla^2 + V + C|\psi|^2)\psi\,. \tag{1}$$

We use scaled harmonic oscillator units (h.o.u.), i.e., for a symmetric harmonic trap with angular frequency ω and particles of mass m, the units of length, time, and energy are $(\hbar/2m\omega)^{1/2}$, ω^{-1}, and $\hbar\omega$, respectively. The nonlinear coefficient $C = 8\pi Na$, where N is the number of atoms per unit length along the z axis and a is the s-wave scattering length. The potential term,

$$V = \tfrac{1}{4}(x^2 + y^2) + \alpha\exp[-\beta x^2 - \beta(y - vt)^2]\,,$$

describes a symmetric harmonic trap with a light-induced "Gaussian" potential barrier, moving with velocity v. We have considered a variety of obstacle parameters but present detailed results for $C = 500$, $\alpha = 30$, and $\beta = 3$. We first calculate the wave function with a stationary object centered at $(0, 0)$ and then, at $t = 0$, begin to propagate the solution for a moving object. The eigenvalue problem $\psi = \phi(x, y)e^{-i\mu t}$ (where μ is the chemical potential and $v = 0$) is easily solved using finite difference methods. With $\alpha = 0$, we find $\mu = 9.003$. The depletion of density in the trap center due to the presence of the obstacle ($\alpha = 30$, $\beta = 3$, $v = 0$) raises the chemical potential to $\mu = 9.208$.

A change in the object potential creates a local disturbance which propagates through the fluid. The time evolution of ψ was determined by the split-operator technique [16]. Instantaneous turn off of the object potential excites sound waves [11], which propagate with speed, $c = \sqrt{2C|\psi|^2}$ ($\sim$4.3 at the peak density). Translation of the object displaces the condensate center of mass [17], and leads to vortex-pair creation as illustrated in Fig. 1. The object and vortex pair are centered at $(0.0, 6.0)$ and $(\pm 2.0, 3.5)$, respectively.

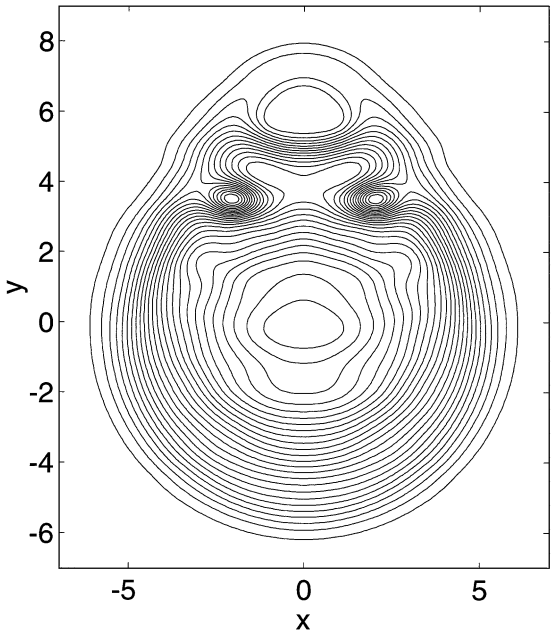

FIG. 1. Contour plot of the condensate density $|\psi(x, y, 3.0)|^2$ for $v = 2.0$. There are 25 contours, equally spaced between 0.0 and 0.0182. The object and vortex pair are centered at $(0.0, 6.0)$ and $(\pm 2.0, 3.5)$, respectively.

Figure 2 shows cuts through the object and vortex pair at $t = 3.0$. The half-width of the vortex core is comparable to the healing length $\lambda \sim C^{-1/4}$. We have simulated the free expansion of the condensate and observe that the vortices also expand, permitting experimental detection using optical imaging.

One can gain insight into the process of vortex formation by studying the evolution of the fluid velocity and the phase of the wave function. Figure 3 shows a quiver plot of the fluid velocity, $\boldsymbol{v}_s = (\psi^* \nabla \psi - \psi \nabla \psi^*)/i|\psi|^2$, in the vicinity of the object, for $t = 3.0$ and $v = 2.0$ (as in Figs. 1 and 2). One sees that vortices are formed in pairs with opposing vorticity, and that the circulating velocity is inversely proportional to distance from the vortex line, as expected. Two pairs are discernible in Fig. 3: one at $y = 3.5$, which corresponds to the density zeros in Fig. 2, and a second at $y = 5.9$ (not visible in Fig. 2, because it has yet to separate from the object). The second pair appears due to the rapid accumulation of phase slip at the edge of the condensate, as discussed below.

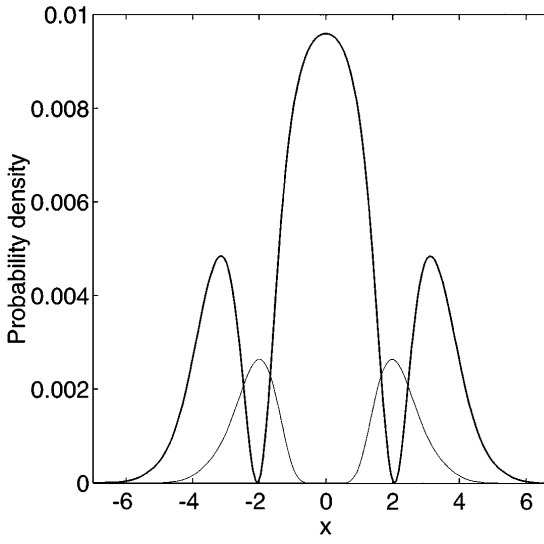

FIG. 2. Plot of the condensate density for $v = 2.0$ passing through the vortex pair $|\psi(x, 3.5, 3.0)|^2$ (bold curve) and the object $|\psi(x, 6.0, 3.0)|^2$.

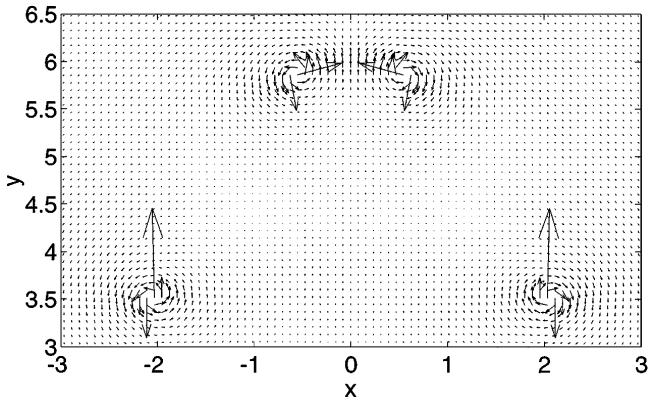

FIG. 3. Plot showing the fluid velocity, $\boldsymbol{v}_s$, in the vicinity of the object, for $t = 3.0$ and $v = 2.0$. v_s in h.o.u. is given by the arrow length/40.

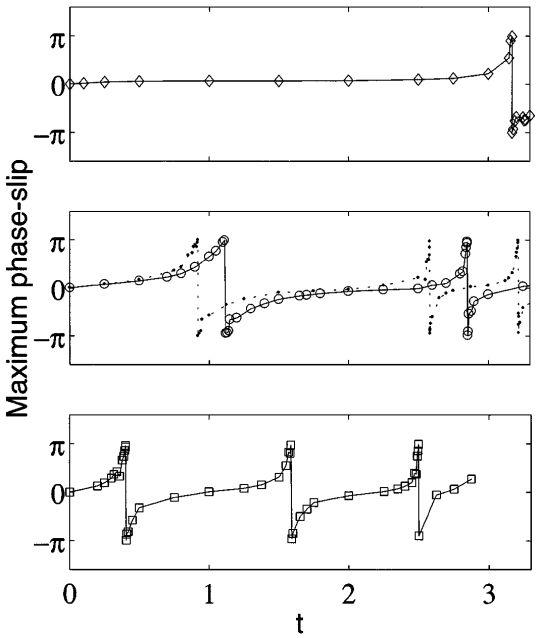

FIG. 4. Time evolution of the maximum phase slip, $\Delta S_{\max}$, for $v = 1.3$ (top), $v = 2.0$ (middle), and $v = 3.0$ (bottom). For $v = 2.0$ we show an additional curve for $C = 200$ (dotted), illustrating that vortices are produced faster when the speed of sound is slower.

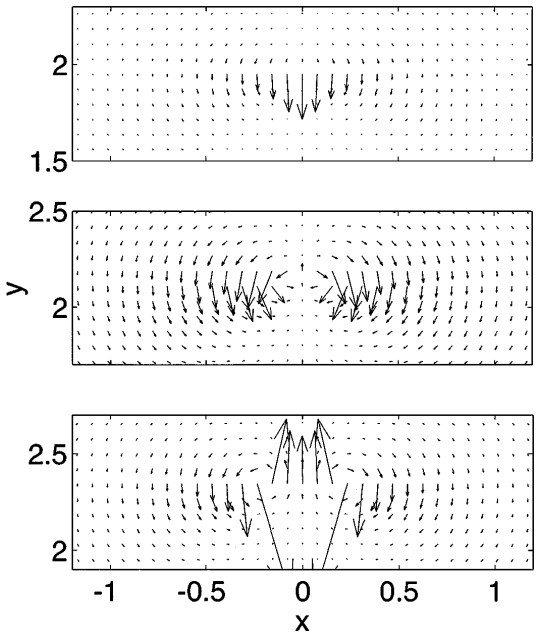

FIG. 5. Plot showing the velocity field in the vicinity of the object for $v = 2.0$, at times spanning the instant of vortex formation: For $t = 1.0$ (top), the on-axis flow is backwards as the fluid attempts to fill the void left by the departing object. At $t = 1.1$ (middle), the fluid begins to skirt around the object and fill the hole with a forward flow. The wave-function nodes (separated by less than one grid point at this stage) are pulled apart due to the gradient in the object potential. By $t = 1.2$ (bottom), their separation is comparable to the healing length, and the pattern of vortex flow is beginning to emerge. v_s in h.o.u. is given by the arrow length/10.

By calculating the wave-function phase, $S(x, y, t)$, one may verify that the phase changes by 2π on circulation of the vortex line [1]. In addition, the evolution of the phase illustrates the time scale for vortex formation. At $t = 0.0$, the phase is uniform. Subsequently, the motion induces a dephasing or "phase slip" centered on the object. The phase slip between two neighboring points along the y axis is defined as $\Delta S(y, t) \equiv \arg\{\psi(0, y + \Delta y, t)\} - \arg\{\psi(0, y, t)\}$, with $-\pi < \arg\{z\} \leq \pi$. The maximum phase slip, $\Delta S_{\max}$, occurs at a y coordinate close to the center of the object. Figure 4 shows a plot of $\Delta S_{\max}$ for different object speeds.

For $v = 2.0$ and 3.0, the phase slip accumulates gradually, reaching a value of π, and then changing sign. The sign change coincides with a reversal of the flow, and may be taken to define the moment of vortex creation. The rate of change of the phase slip is related to the speed of sound which determines the time scale over which the condensate can respond to an external perturbation. For a smaller nonlinear coefficient, i.e., lower sound velocity, the phase slip accumulates more rapidly and the vortex pair is created earlier (compare curves for $C = 200$ and $C = 500$ in Fig. 4). After the vortices are created, the phase slip builds again until a second pair forms, and so on. For low object speed (e.g., $v = 1.3$, upper plot in Fig. 4) the phase slip initially saturates and then increases towards the edge of the condensate, where the density and hence the local speed of sound are lower. This explains the sudden formation of a vortex pair as the object leaves the condensate (e.g., the second pair for $v = 2.0$ appearing in Figs. 3 and 4). For $v = 3.0$, a third pair is created at $t = 2.5$: The object is still surrounded by condensate at this time because of a motion-induced "stretching."

The evolution of the velocity field while the vortex is forming is shown in Fig. 5. One sees that the vortices emerge from a point and then separate. For longer times, they drift towards the edge of the condensate.

In summary, we have solved the time-dependent NLSE in 2D to simulate the flow of an object through a dilute Bose-Einstein condensate trapped in a harmonic well. We find that the vortices emerge from a point close to the center of the object, and that the vortex shedding frequency is higher when the speed of sound is lower. We expect that our 2D simulations should correspond to the 3D case, where an oblate spheroid condensate is pierced by a tightly focused laser beam.

A complete description of dilute atomic vapors should also include the effects of the noncondensate density, finite temperature, and dissipation. To what extent the NLSE provides an accurate description of vortex formation requires quantitative comparison between simulation and experiment. Such a comparison will provide the focus for future work.

Financial support was provided by the Nuffield Foundation and the EPSRC.

[1] P. Nozières and D. Pines, *The Theory of Quantum Liquids* (Addison-Wesley, Redwood City, 1990), Vol. II.
[2] R. P. Feynman, Prog. Low Temp. Phys. **1**, 17 (1955).
[3] M. H. Anderson, J. R. Ensher, M. R. Matthews, C. E. Wieman, and E. A. Cornell, Science **269**, 198 (1995).
[4] K. B. Davis, M. O. Mewes, M. R. Andrews, N. J. van Druten, D. S. Durfee, D. M. Kurn, and W. Ketterle, Phys. Rev. Lett. **75**, 3969 (1995).
[5] C. C. Bradley, C. A. Sackett, and R. G. Hulet, Phys. Rev. Lett. **78**, 985 (1997).
[6] V. L. Ginzburg and L. P. Pitaevskii, Sov. Phys. JETP **7**, 858 (1958); E. P. Gross, J. Math. Phys. **4**, 195 (1963).
[7] D. S. Jin, J. R. Ensher, M. R. Matthews, C. E. Wieman, and E. A. Cornell, Phys. Rev. Lett. **77**, 420 (1996).
[8] M.-O. Mewes, M. R. Andrews, N. J. van Druten, D. M. Kurn, D. S. Durfee, C. G. Townsend, and W. Ketterle, Phys. Rev. Lett. **77**, 988 (1996).
[9] R. J. Dodd, M. Edwards, C. W. Clark, and K. Burnett, Phys. Rev. A **57**, R32 (1998), and references therein.
[10] M. R. Andrews, C. G. Townsend, H.-J. Miesner, D. S. Durfee, D. M. Kurn, and W. Ketterle, Science **275**, 637 (1997).
[11] M. R. Andrews, D. M. Kurn, H.-J. Miesner, D. S. Durfee, C. G. Townsend, S. Inouye, and W. Ketterle, Phys. Rev. Lett. **79**, 547 (1997).

[12] D. M. Stamper-Kurn, M. R. Andrews, A. P. Chikkatur, S. Inouye, H.-J. Miesner, J. Stenger, and W. Ketterle, Phys. Rev. Lett. **80**, 2027 (1998).
[13] H.-J. Miesner and W. Ketterle, Solid State Commun. (to be published).
[14] T. Frisch, Y. Pomeau, and S. Rica, Phys. Rev. Lett. **69**, 1644 (1992).
[15] A. C. Newell and Y. Pomeau, Physica (Amsterdam) **87D**, 216 (1995).
[16] Most of the calculations were performed using a square box of side 10 h.o.u. divided into a grid of 256×256 points. A larger grid (20 h.o.u., 512×512) was used to check for edge effects. More details of the numerical methods employed are discussed elsewhere [B. Jackson, J. F. McCann, and C. S. Adams (to be published)].
[17] The center-of-mass motion provides a useful diagnostic: The initial acceleration is v divided by the integration time step; after a few steps the solution is only sensitive to v and, when the object leaves the condensate, the center of mass oscillates at the trap frequency.